

# Sulforaphane: a naturally occurring mammary carcinoma mitotic inhibitor, which disrupts tubulin polymerization

Steven J.T.Jackson and Keith W.Singletary<sup>1</sup>

Department of Food Science and Human Nutrition, University of Illinois, 467 Bevier Hall—M/C 182, 905 S. Goodwin Ave., Urbana, IL 61801, USA

<sup>1</sup>To whom correspondence should be addressed  
Email: kws@uiuc.edu

**Sulforaphane (SUL), an isothiocyanate found in broccoli and other cruciferous vegetables, has been shown to induce phase II detoxification enzymes, inhibit chemically induced mammary tumors in rats, and more recently to induce cell cycle arrest and apoptosis in cancer cells of the colon. Here, we provide evidence that SUL also acts as a breast cancer anti-proliferative agent. The BALB/c mouse mammary carcinoma cell line F3II was treated with SUL at concentrations up to 15  $\mu$ M and examined for markers of cell cycle arrest and apoptosis. Treatment of asynchronous F3II cells with 15  $\mu$ M SUL resulted in G<sub>2</sub>/M cell cycle arrest, elevated p34<sup>cdc2</sup> (cdc2) kinase activity, Bcl-2 down-regulation, evidence of caspase activation, and aggregation of condensed nuclear chromatin. Subsequent exposure of synchronized cells to 15  $\mu$ M SUL resulted in elevated numbers of prophase/prometaphase mitotic figures, indicating cell cycle progression beyond G<sub>2</sub> and arrest early within mitosis. Moreover, cells treated with 15  $\mu$ M SUL displayed aberrant mitotic spindles, and higher doses of SUL inhibited tubulin polymerization *in vitro*. In addition, BALB/c mice injected s.c. with F3II cells and subsequently injected daily i.v. with SUL (15 nmol/day for 13 days) developed significantly smaller tumors (~60% less in mass) than vehicle-treated controls. Western blot analysis of tumor proteins demonstrated significantly ( $P < 0.05$ ) reduced PCNA and elevated PARP fragmentation in samples from animals dosed with SUL. Taken together, these results indicate that SUL has mammary cancer suppressive actions both in cell culture and in the whole animal. Inhibition of mammary carcinogenesis appears in part to involve perturbation of mitotic microtubules and early M-phase block associated with cdc2 kinase activation, indicating that cells arrest prior to metaphase exit.**

## Introduction

Sulforaphane [1-isothiocyanato-4-(methyl-sulfinyl)butane] (SUL) is an isothiocyanate found in broccoli and other cruciferous vegetables that forms following the hydrolysis of the glucosinolate compound glucoraphanin via the action of thioglucoside glucohydrolase (1). SUL is of interest to the field of diet and breast cancer research for several reasons. First, it exists as a component of commonly consumed vegetables and is especially abundant in broccoli (2). In some epidemiologic studies, vegetable intake has been reported to be inversely associated

with breast cancer risk (3–5). Secondly, it has been shown to inhibit the formation of chemically induced mammary tumors in rats (6). Lastly, it is an inducer of phase II detoxification enzymes (7) and a competitive inhibitor of the phase I enzyme cytochrome P450 isozyme 2E1 (CYP2E1), an enzyme participating in carcinogen activation (8). Thus, considerable attention has focused on its potential as an inhibitor of cancer initiation. However, SUL recently has been shown to inhibit neoplastic cell proliferation, block cell cycle progression at G<sub>2</sub>/M, induce apoptosis and modulate signal transduction pathways, suggesting that it may be an effective inhibitor of neoplastic cell proliferation and cancer promotion/progression (9).

Evidence for SUL's inhibition of cell proliferation and induction of apoptosis comes from the publication of Gamet-Payrastré *et al.* (9). In these studies, exposure of HT29 human colon cancer cells to 15  $\mu$ M SUL resulted in cell cycle arrest at G<sub>2</sub>/M. SUL-treated cells exhibited over-expression of the apoptosis inducer Bax, a decrease in mitochondrial cytochrome *c*, an increase in cytosolic cytochrome *c*, and presence of the proteolytic cleavage fragment of PARP, while the apoptosis repressor Bcl-2 was unchanged. Similar cellular responses have been observed with phenethyl isothiocyanate (PEITC), which like SUL exists as a glucosinolate in a number of cruciferous vegetables. PEITC induced apoptosis in mouse epidermal JB6 cells through a p53-dependent pathway (10) and induced both caspase-3-like activity and apoptosis in HeLa cells in a time- and dose-dependent manner (11). The activity of the cyclin-dependent kinase p34<sup>cdc2</sup> or cdc2 (CDK1) has been identified as being important in controlling not only passage of the cell cycle from G<sub>2</sub> to mitosis, but also for initiation of cell death pathways (12–15). Specifically, activation of cdc2 is generally thought to involve phosphorylation at threonine 161 (16–19), binding of cyclin B1 (18,20–22) and dephosphorylation at both threonine 14 and tyrosine 15 (18,21). Phosphorylation and subsequent dephosphorylation of cdc2 at threonine 14 and tyrosine 15 occurs, respectively, via the action of Wee1 (tyrosine kinase) and Myt1 (threonine and tyrosine kinase) kinases (21,23–29) and cdc25C phosphatase (30–32). An active cdc2 then phosphorylates a number of cellular substrates such as H1 histone, nuclear lamins, vimentin, caldesmon and nucleolin, which allow progression into and through mitosis (33–41). The end of mitosis and return to G<sub>1</sub> phase is marked by inactivation of cdc2, which occurs via dephosphorylation of threonine 161 (catalysed at least in part by type 1 phosphatases) (42) and degradation of cyclin B1 (43).

Of additional interest is the recognition that inappropriate activation of cdc2 can lead to a form of cell death known as 'mitotic catastrophe' (14,15). For example, Shi *et al.* demonstrated a requirement for increased cdc2 activity in fragmentin-2-induced apoptosis in the murine mammary carcinoma cell line FT210 (15). Moreover, Fotedar *et al.*, using a murine T-cell hybridoma (A11 cells), detected that activation of apoptosis was associated with cdc2 dephosphorylation, increased

**Abbreviation:** SUL, sulforaphane.

cdc2 kinase activity, and arrest of the cell cycle at G<sub>2</sub>/M (44). Thus, the activity of cdc2 at the G<sub>2</sub>/M transition is an important factor in determining whether the cell cycle arrests prior to or during mitotic progression, and/or whether apoptosis is initiated. Considerable progress has been made in characterizing the events controlling programmed cell death. In particular, the Bcl-2 family of gene products has been shown to be important in regulating programmed cell death, with some members serving as apoptosis repressors (e.g. Bcl-2, Bcl-X<sub>1</sub>, Bcl-w) while others are apoptosis inducers (e.g. Bax, Bcl-X<sub>s</sub>, Bad) (45). The relative abundance of homo- and heterodimers of Bcl-2 proteins in the mitochondrion determines whether cell death is induced or repressed (46–48). The Bax protein translocates from the cytosol to mitochondrial membranes and is thought to be involved in subsequent loss of mitochondrial membrane potential, release of cytochrome *c*, and activation of the caspase cascade (49–52). Caspases 3 and 7, for example, encourage apoptosis by cleaving cellular substrates such as the DNA repair protein poly(ADP-ribose) polymerase (PARP), the 70-kDa protein component of the U1-ribonucleoprotein, and the DNA-dependent protein kinase (11,53,54).

In light of SUL's reported actions in inhibiting proliferation of colon cancer cells, we initiated the present studies to characterize the effect of SUL on breast cancer cell proliferation and apoptosis in a mouse carcinoma cell line. Specifically, mechanisms for SUL's anti-proliferative and proapoptotic action were identified, and its efficacy to inhibit carcinoma cell multiplication *in vivo* was tested by syngeneic transplantation.

## Materials and methods

### Cell culture

F3II cells are a sarcomatoid mammary carcinoma cell line derived from a clonal subpopulation of a BALB/c mouse mammary adenocarcinoma, and were kindly provided by Dr Daniel Alonso (Buenos Aires, Argentina). Stock cells were routinely cultured in MEM containing 5% heat-inactivated fetal bovine serum at 37°C under a 5% CO<sub>2</sub> atmosphere, and the medium was changed every 48 h. Unless stated otherwise, experiments were conducted in 75 cm<sup>2</sup> Corning tissue culture flasks (seeding density = 5 × 10<sup>5</sup> cells/flask), and the culture medium was changed 24 h after seeding. All cell culture experiments were carried out with a minimum of three samples per group, and D,L-SUL (97%, ICN) or DMSO (vehicle, 0.1%) was administered 36–48 h after seeding.

### Cell growth assay

Cells were seeded at a density of 4 × 10<sup>3</sup> cells/cm<sup>2</sup> in 25 cm<sup>2</sup> Corning tissue culture flasks. Cultures were exposed to increasing dosages of SUL or DMSO for 48 h prior to harvesting (via trypsinization) and counting (via hemocytometer) of both cells adherent to the culture flask and those floating in the culture medium.

### [<sup>3</sup>H]Thymidine incorporation assay of DNA synthesis

Cells were seeded at a density of 6.25 × 10<sup>3</sup> cells/cm<sup>2</sup> in Costar 48-well plates. Two days after seeding, cultures were exposed to increasing dosages of SUL or DMSO in the presence of [<sup>3</sup>H]thymidine (1 μCi). After 24 h, the medium was removed and the cells washed with PBS, treated with 5% trichloroacetic acid (15 min), and the precipitate washed with absolute methanol and, after 5 min, dissolved in 88% formic acid (Fisher, Pittsburgh, PA) for 5 min at room temperature. The samples were measured in a Beckman LS6500 Scintillation Counter in the presence of ScintiVerse SX16-4 (Fisher) counting cocktail.

### Cell cycle analysis and quantification of mitotic figures

Cells were treated with either SUL or DMSO and, at the indicated times, harvested via trypsinization. The cells were then washed with PBS, fixed in 70% ethanol (at least 12 h, 4°C), washed again with PBS, and resuspended in modified Vindelov's DNA staining solution (0.1 mg/ml RNase A, 0.1% NP-40, 0.25 mg/ml propidium iodide, in PBS) at a density of ~10<sup>6</sup> cells/ml. Fluorescence was then measured 1 h later using a Coulter XL Flow Cytometer.

In order to quantify cells in mitosis, cells were first plated (1 × 10<sup>6</sup> cells/75 cm<sup>2</sup> culture flask) and, 24 h later, synchronized at G<sub>1</sub>/S (1 mM hydroxyurea for 12 h), prior to washing with fresh culture medium, medium replacement, and treatment with 15 μM SUL or DMSO. Once the exposure time had elapsed, cells were harvested via trypsinization, washed with PBS, resuspended in PBS and cytospun onto microscope slides. Cells were then stained with Wright-Giemsa dye, and the percentage of mitotic figures determined by analysing a minimum of 10 cells in each of six fields per slide under light microscopy.

### Immunofluorescence staining

Cells were plated on 12 mm round glass coverslips, and 36 h later exposed to 15 μM SUL or DMSO for 36 h. After washing once with PBS, cells were fixed with glutaraldehyde (1% in PBS, for 10 min at room temperature) followed by sodium borohydride (1 mg/ml in PBS, twice for 10 min each). Cells were then rinsed three times with PBS, permeabilized with wash buffer (0.1% Triton X-100, 1% BSA in TBS) for 10 min, and incubated with a monoclonal antibody to α-tubulin (Oncogene Research Products, San Diego, CA, CP06) for 30 min at room temperature. Following five washes with wash buffer, cells were incubated with a FITC-conjugated goat anti-mouse secondary antibody (Santa Cruz Biotechnology, Santa Cruz, CA, sc-2078) and the DNA counterstained with DAPI (10 μg/ml) for 30 min at room temperature. Finally, samples were washed again five times with wash buffer, washed once with dH<sub>2</sub>O, mounted on microscope slides with mounting medium (ICN, #622701), and analyzed by fluorescence microscopy.

### In vitro tubulin polymerization assay

Bovine brain tubulin (>99% pure, Cytoskeleton, #BK006) was incubated in the presence of SUL (*n* = 3/dose group), the direct microtubule depolymerizing agent nocodazole, or DMSO (vehicle) in a 96-well plate at 37°C. Absorbance readings were taken at 340 nm using a Molecular Devices Spectra Max Plus plate reader each minute for 1 h according to kit instructions.

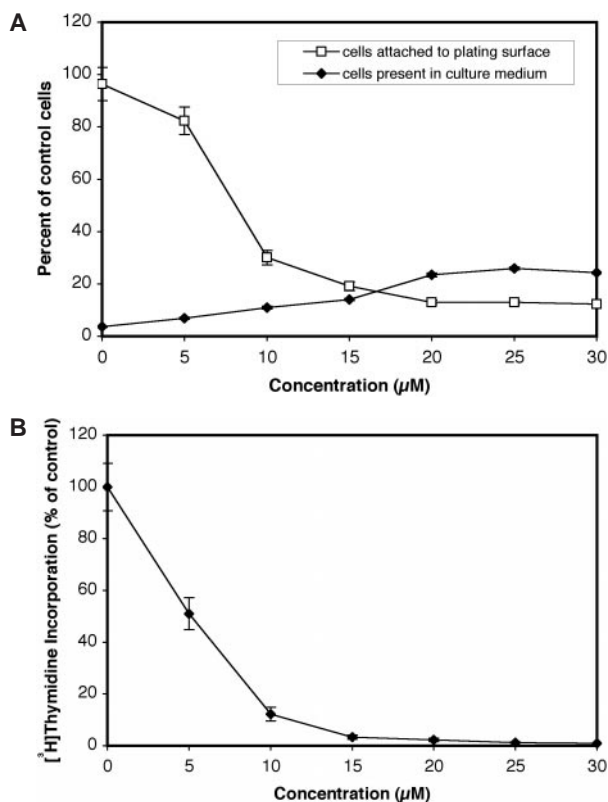


**Fig. 1.** Effect of sulforaphane on cell proliferation. (A) Cultures (*n* = 4/group) were exposed to increasing dosages of SUL for 48 h prior to harvesting and cytometry of both cells adherent to the culture flask and those floating in the culture medium. Mean values (±SE) are expressed as the percentage of control (attached + floating) cells. (B) Cultures (*n* = 6/group) were exposed to increasing dosages of SUL in the presence of [<sup>3</sup>H]thymidine (1 μCi) for 24 h. Mean values (±SE) are expressed as the percentage of control group [<sup>3</sup>H]thymidine incorporation. Data are representative of two independent experiments.

*Western blot analysis*

Cells were washed twice with TBS, harvested in ice-cold lysis buffer [1% SDC, 1% Triton X-100, 0.01% SDS, 150 mM NaCl, 50 mM Tris (pH 7.5), 0.5 mM EDTA, 50 mM NaF, 10 mM NaPP<sub>i</sub>, 0.5 mM Na<sub>3</sub>VO<sub>4</sub>, 1 mM PMSF, 0.02 mg/ml aprotinin, 0.02 mg/ml leupeptin, 0.02 mg/ml pepstatin], sonicated and centrifuged (15 000 *g* for 15 min at 4°C). The supernatant was then assayed for total protein (BCA, Pierce, Rockford, IL), and aliquots of equal protein concentration were fractionated by SDS-PAGE (7.5%) and transferred to nitrocellulose membranes. The membranes were blocked and then incubated with a polyclonal phospho-specific antibody to histone H1 (Upstate Biotechnology, Lake Placid, NY, #06-597). Following incubation with an HRP-conjugated secondary antibody (Santa Cruz Biotechnology) from the appropriate species, immunodetection was carried out using chemiluminescence (ECL, Amersham Life Sciences, Piscataway, NJ). Exposed X-ray film was then scanned into Adobe Photoshop, and densitometric analysis was performed on an Apple Macintosh G4 computer using the public domain NIH Image program (developed at the US National Institutes of Health and available on the Internet at <http://rsb.info.nih.gov/nih-image/>). Similar procedures were utilized for detecting levels of expression of cdc2 (Santa Cruz Biotechnology, sc-54), Bcl-2 (sc-492), PCNA (sc-56) and PARP (sc-7150 for cell culture, and Cell Signaling Technology, Beverly, MA, #9542 for tumor samples). Equal loading of total protein was confirmed by reprobing membranes for actin (sc-1616).

*In vitro assay of p34<sup>cdc2</sup> kinase activity*

Cells were washed twice with TBS, harvested in ice-cold lysis buffer [1% Triton X-100, 150 mM NaCl, 50 mM Tris (pH 7.5), 0.5 mM EDTA, 50 mM NaF, 10 mM NaPP<sub>i</sub>, 10 mM β-glycerophosphate, 0.5 mM Na<sub>3</sub>VO<sub>4</sub>, 1 mM PMSF, 0.02 mg/ml aprotinin, 0.02 mg/ml leupeptin, 0.02 mg/ml pepstatin], and centrifuged (15 000 *g* for 15 min at 4°C). After pre-clearing the supernatant for 1 h with IgG<sub>2a</sub> (Oncogene Research Products, OB02; 1 μg) and Protein A-agarose (sc-2001), each sample was assayed for total protein content. Aliquots of each lysate containing 250 μg total protein were then brought to equal volume (0.75 ml in lysis buffer) in 1.5 ml Eppendorf tubes.

Immunoprecipitation was carried out using mouse monoclonal anti-p34<sup>cdc2</sup> antibody (sc-54; 1 μg) and Protein A-agarose at 4°C overnight. Immune complexes were then washed twice with kinase buffer [50 mM Tris (pH 7.5), 10 mM MgCl<sub>2</sub>, 1 mM DTT] and pelleted by centrifugation. The reactions were initiated by the addition of 30 μl kinase buffer containing 10 μM ATP, 10 μg histone H1, and 5 μCi [γ-<sup>32</sup>P]ATP. Following a 30 min incubation at 30°C, the reactions were terminated by the addition of 10 μl sample buffer [62.5 mM Tris-HCl (pH 6.8), 10% glycerol, 2% (w/v) SDS, 5% β-mercaptoethanol in dH<sub>2</sub>O containing a trace of bromophenol blue]. The reaction products were resolved by 7.5% SDS-PAGE and transferred to nitrocellulose membrane. Kinase activity was then visualized by autoradiography and quantified by densitometric analysis.

*Chromatin condensation analysis*

Cells were plated at a density of 1 × 10<sup>4</sup> cells/well on chamber slides (4.2 cm<sup>2</sup>; Nalge Nunc, Naperville, IL) and allowed to grow for 2 days prior to treatment with 15 μM SUL or DMSO. After treating for 36 h, cells were washed twice with PBS, fixed with methanol/ethanol (1/1, ice-cold, 10 min at -20°C), washed again with PBS (room temperature), and stained with Hoechst 33342 (10 μg/ml in PBS, 15 min in the dark). Cells were then washed (three times) with PBS, and analyzed by fluorescence microscopy. Phase contrast images were also captured of identical fields scored for fluorescent chromatin condensation in order to allow for quantification of total cells per field and calculation of the percentage of cells per sample displaying condensed nuclear chromatin.

*Caspase-3-like activity assay*

Cells were harvested via trypsinization, followed by measurement of caspase-3-like activity using a colorimetric caspase-3/7 substrate (Ac-DEVD-pNA) according to kit instructions (Calbiochem, San Diego, CA, No. 235419). Briefly, cells were counted, washed with PBS, and lysed in cell lysis buffer (2 × 10<sup>7</sup> cells/ml) prior to assay for total protein in each sample. Cell extract, blank and inhibitor-treated cell extract aliquots were prepared in a 96-well microtiter plate, and absorbance at 405 nm was recorded at 10 min intervals for

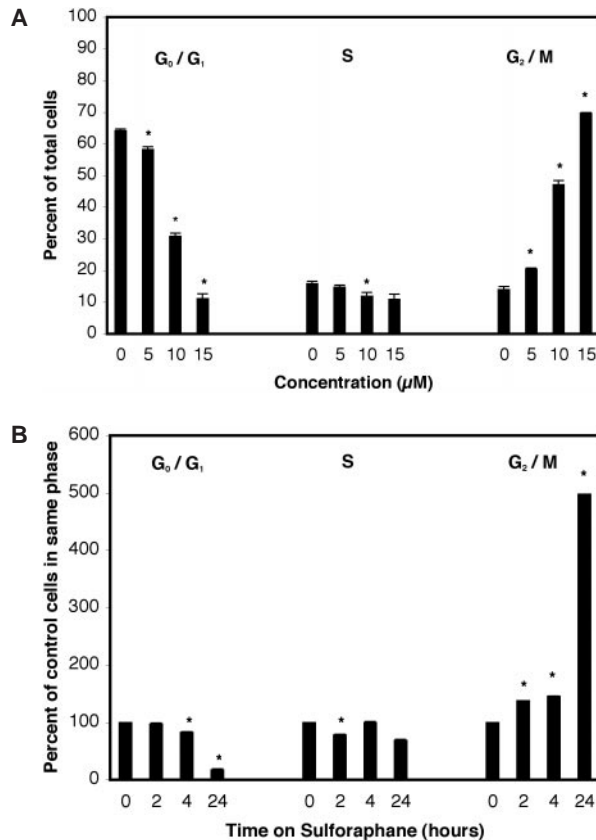


**Fig. 2.** Effect of SUL on cell cycle distribution. Cultures ( $n = 3$ /group) were exposed to either (A) increasing dosages of SUL for 24 h, or (B) 15 μM SUL for the indicated times, prior to analysis by flow cytometry. Mean values ( $\pm$  SE) are expressed as the percentage of total cells in all phases (A) and the percentage of control cells determined for each phase (B). Data are representative of two independent experiments.

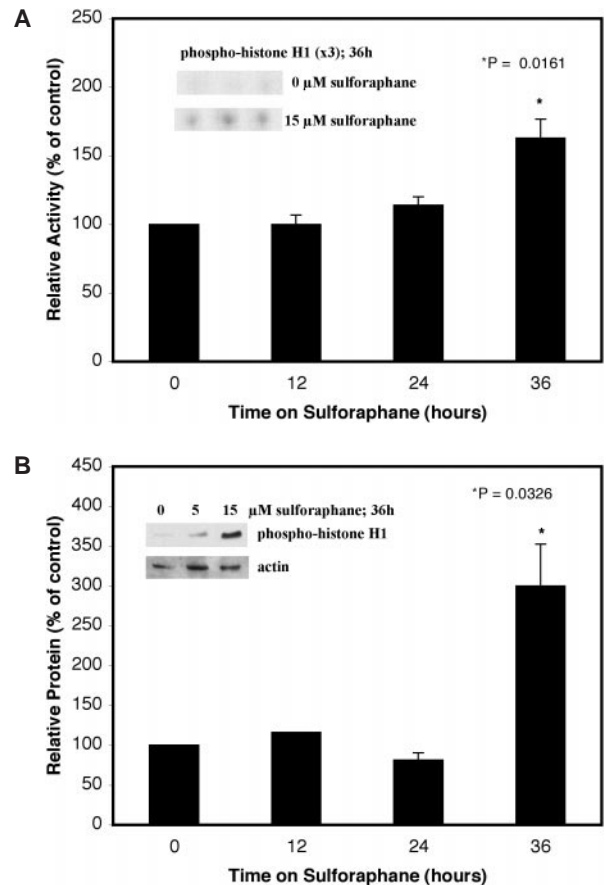


**Fig. 3.** Effect of SUL on cdc2 kinase activity. Cultures ( $n = 3-4$ /group) were exposed to 15 μM SUL or DMSO (vehicle) for the indicated times prior to determination of cdc2 kinase activity *in vitro* (A) or *in vivo* (B). Data are representative of two independent experiments.

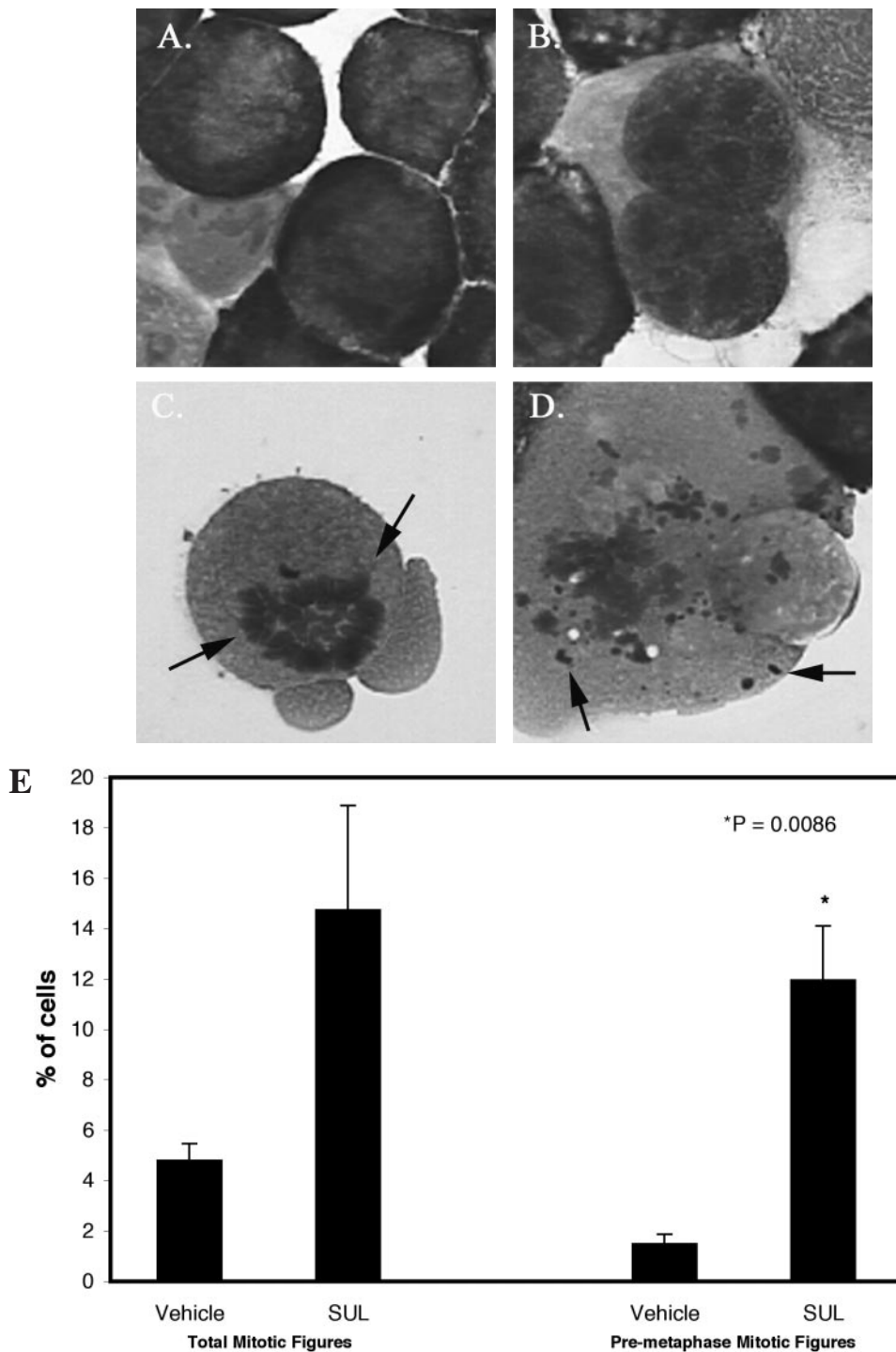


**Fig. 4.** Effect of SUL on mitotic progression in synchronized F3II cells. Cultures ( $n = 3/\text{group}$ ) were exposed to 15  $\mu\text{M}$  SUL (C and D) or DMSO (vehicle; A and B) for 12 h prior to Wright-Giemsa staining. The figure represents the abundance of mitotic figures in a prophase or prometaphase-like state (C, see arrows), as well as aberrant, fragmented nuclear DNA (D, see arrows), while control cells cycle beyond metaphase (B). (E) Quantification of both total and pre-metaphase mitotic figures. Data are representative of two independent experiments.

2 h. Specific caspase-3-like activity was calculated based on the mean slope ( $A_{405}$  versus time) of three replicates in each group and total protein (pmol/min/ $\mu\text{g}$  protein).

*Intravenous SUL and the growth of F3II cells in vivo*

Female Balb/C mice (Harlan, Indianapolis, IN) at 10 weeks of age were housed individually in stainless steel cages and maintained on a 12 h light/12 h dark cycle (lights on at 05:00) with AIN-93G diet and water available *ad libitum*. All procedures were carried out in accordance with a protocol approved by the

Institutional Animal Care Committee. F3II cells were administered to both the right and left flank regions of mice via s.c. injection ( $2 \times 10^4$  cells per injection site). Five days later, lateral tail vein injections of SUL (15 nmol) or sterile 0.9% NaCl (vehicle) were performed daily (days 1–13, between 06:00 and 09:00). On day 14, all animals were killed (by  $\text{CO}_2$  asphyxiation), the localized tumors excised, and groups examined for differences in mean tumor mass. Following the analysis of tumor mass data, two subgroups of control and SUL-treated tumor samples ( $n = 3\text{--}4$ ) of mass within  $\pm 1$  SD of the respective group means were chosen randomly for western blot analysis.

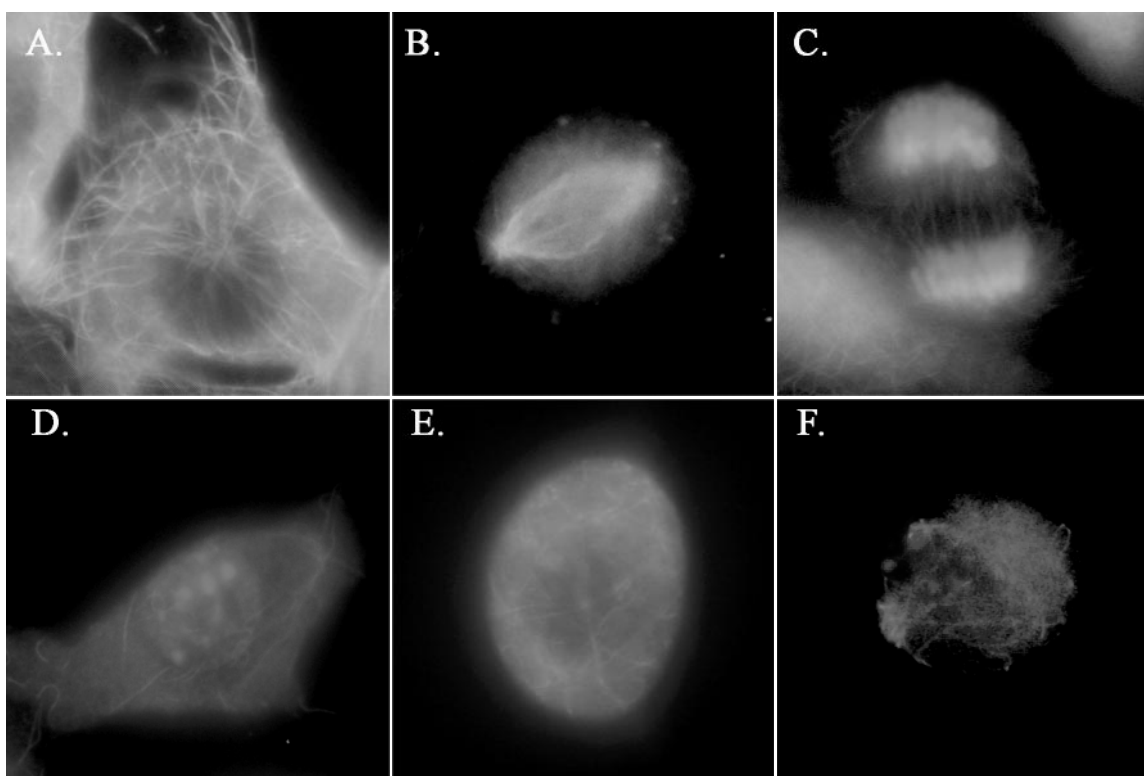


**Fig. 5.** Effect of SUL on F3II cell microtubule polymerization. Microtubules (green) and DNA (blue) were stained in cultures exposed to either 15  $\mu\text{M}$  SUL (D, E and F) or DMSO (vehicle, A, B and C) for 36 h. While cytoplasmic microtubules of asynchronous interphase cells appeared generally intact (D and E), SUL treatment led to aberrant and mildly depolymerized mitotic microtubule spindles (F), while control cells cycled beyond metaphase (C). Data are representative of two independent experiments.

Briefly, tumors from both left and right regions were homogenized together in lysis buffer, sonicated and centrifuged twice, yielding the whole cell lysate. Samples were then assayed for total protein and analyzed as described in the previous section.

#### Statistical analysis

Treatment group means were compared to the respective control group means by *t*-test for independent samples and the accompanying test for homogeneity of variance (The SAS System, SAS Institute). Statistically significant differences were established at  $P < 0.05$  and are depicted in figures by an asterisk (\*).

## Results

### SUL suppresses mammary cancer cell proliferation

Treatment of F3II cells with SUL at doses up to 30  $\mu\text{M}$  inhibited cell proliferation in a dose-dependent manner. Within 48 h, SUL treatment clearly reduced both the number of cells attached to the plating surface as well as the total number of cells present in culture. Also, there was a modest accumulation of cells floating in the culture medium (Figure 1A). Similarly, 24 h of SUL treatment reduced DNA synthesis (Figure 1B), with an  $\text{IC}_{50}$  value of  $\sim 5 \mu\text{M}$ . Since concentrations in excess of 15  $\mu\text{M}$  possessed little, if any, added activity in either assay, this dose was chosen as the maximum concentration for use in all subsequent cell culture dose-response experiments, as well as for characterization of time-dependent actions of SUL.

### SUL induces early mitotic arrest

Cells treated with SUL accumulated within the  $\text{G}_2/\text{M}$  phase of the cell cycle, in both a dose- and time-dependent manner (Figure 2). Within 24 h, compared with controls, treatment of

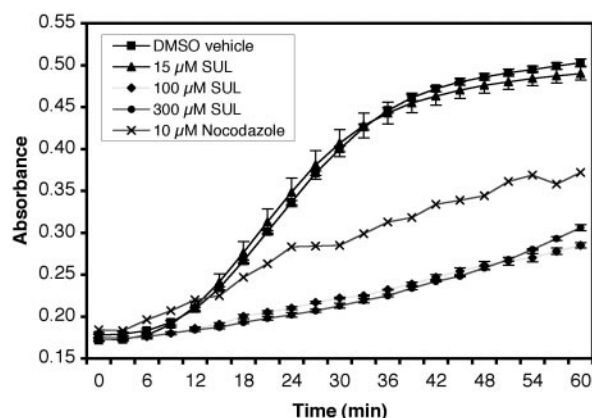


**Fig. 6.** Effect of SUL on tubulin polymerization *in vitro*. Purified bovine brain tubulin was incubated in the presence of the indicated SUL concentrations ( $n = 3/\text{group}$ ), nocodazole, or DMSO (vehicle) at  $37^\circ\text{C}$ , and absorbance readings were recorded each minute for 1 h. For clarity, mean data ( $\pm\text{SE}$ ) are presented at 3-min intervals. Data are representative of two independent experiments.

cells with 15  $\mu\text{M}$  SUL resulted in a 5-fold increase in the proportion of cells within  $\text{G}_2/\text{M}$ , while a significant  $\text{G}_2/\text{M}$  accumulation was observed as early as 2 h following SUL administration. Within 36 h, both *in vitro* and *in vivo* assays of *cdc2* kinase activity indicated significant activity elevations (Figure 3), while total *cdc2* protein remained unaffected (data not shown). Moreover, Wright-Giemsa staining of synchronized F3II cultures exposed to 15  $\mu\text{M}$  SUL for 12 h demonstrated an abundance of mitotic figures in a prophase or prometaphase-like state (individual chromosomes condensed

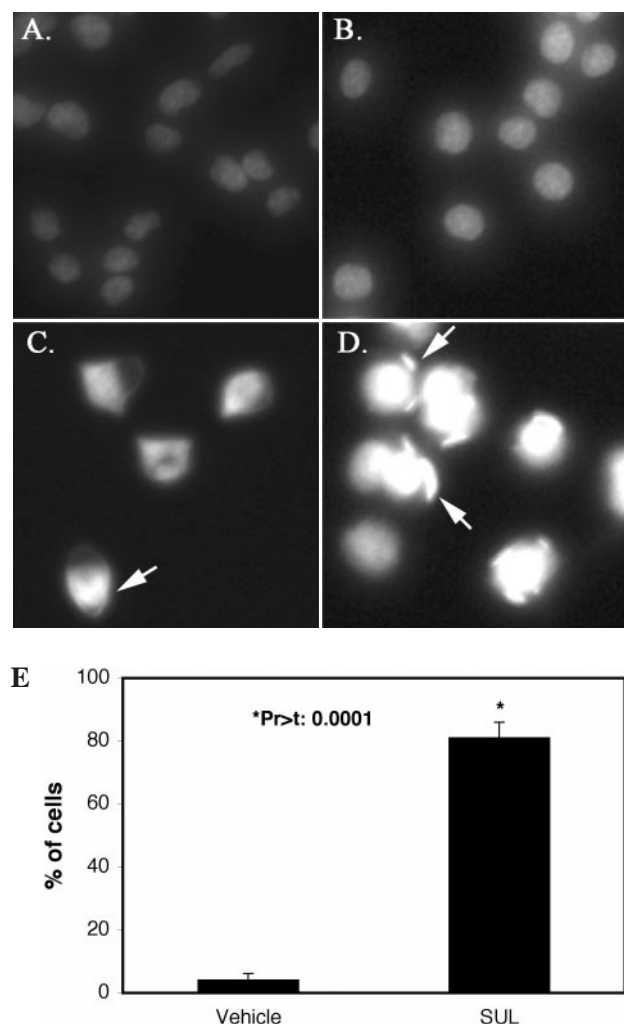


**Fig. 7.** Effect of SUL on nuclear chromatin. Cultures ( $n = 3/\text{group}$ ) were exposed to 15  $\mu\text{M}$  SUL (C and D) or DMSO (A and B) for 36 h prior to staining with Hoechst 33342. The figure represents the abundance of cells displaying aggregates of condensed nuclear chromatin in the region of the nuclear membrane (C and D, see arrows). (E) Quantification of cells displaying nuclear chromatin condensation.

and distinguishable, yet not aligned at the equatorial plate), as compared with vehicle-administered controls (Figure 4). While SUL-treated cultures also exhibited elevated numbers of total mitotic figures, the effect was statistically significant only with quantification of the early, pre-metaphase mitotic figures, as control samples displayed some later mitotic stages (Figure 4E). Variability in the number of these other mitotic figures probably contributed to lack of statistical significance with regard to total mitotic figures. Tubulin staining of F3II cells demonstrated that SUL treatment did not result in generalized depolymerization of cellular microtubules (Figure 5), yet mitotic cells displayed aberrant and mildly depolymerized spindles within 36 h of treatment with 15  $\mu\text{M}$  SUL (Figure 5F).

#### *SUL inhibits tubulin polymerization in vitro*

SUL doses  $>15 \mu\text{M}$  were found to interfere with polymerization of purified tubulin *in vitro* (Figure 6). Indeed, these relatively high doses of SUL (100 and 300  $\mu\text{M}$ ) inhibited gross tubulin polymerization to a similar extent as that observed with the direct microtubule depolymerizing agent nocodazole.

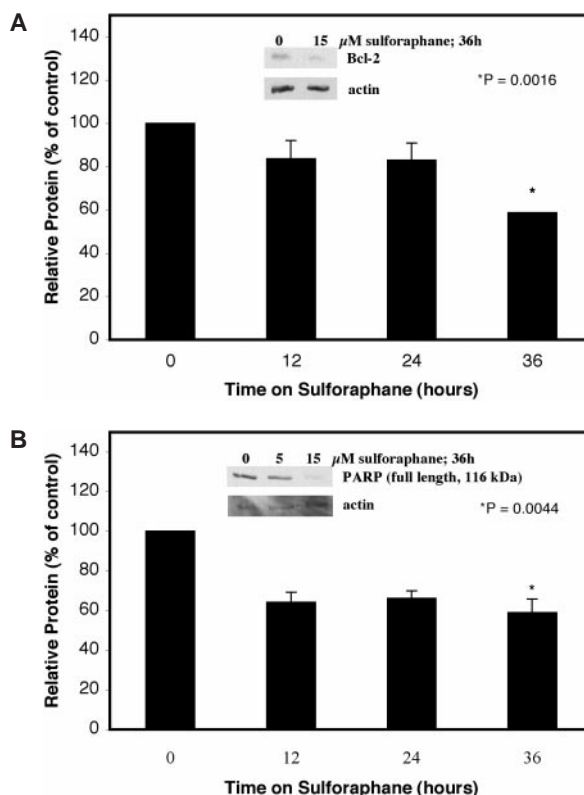


**Fig. 8.** Effect of SUL on apoptosis markers in F3II cells. Bcl-2 protein (A) and full-length PARP (B) were significantly reduced ( $P < 0.05$ ) within 36 h of SUL treatment. Data are representative of two independent experiments.

#### *SUL induces apoptosis*

Within 36 h, Hoechst 33342 staining of cells exposed to 15  $\mu\text{M}$  SUL demonstrated aggregation of condensed nuclear chromatin, notably at the region of the nuclear membrane (Figure 7). Plasma membrane blebbing, as well as aberrant, fragmented DNA (Figure 4D), was also observed in synchronized F3II cells exposed to 15  $\mu\text{M}$  SUL. In addition, western blot analysis of whole cell lysates exhibited significant reductions of the apoptosis repressor Bcl-2 and the DNA repair protein PARP within 36 h following administration of 15  $\mu\text{M}$  SUL (Figure 8). Also, caspase-3-like activity was found to be elevated within 2 h (and peaked within 24 h) following treatment with 15  $\mu\text{M}$  SUL (data not shown).

#### *Intravenous SUL inhibits F3II cell tumor development in BALB/c mice*

BALB/c mice injected s.c. with F3II cells and subsequently injected daily i.v. with SUL (15 nmol) developed significantly smaller tumors (~60% less in mass) than vehicle-treated controls (Figure 9A). No overt signs of toxicity were observed following SUL administration. Also, western blot analysis of tumor protein samples indicated that the proliferation marker PCNA was significantly reduced (Figure 9B), while PARP fragment was strongly elevated (Figure 9C) in animals exposed to SUL.

## Discussion

The present report provides the first evidence of SUL-induced mitotic arrest and apoptosis in mammary carcinoma cells. We observed in cell culture that SUL decreased Bcl-2 protein

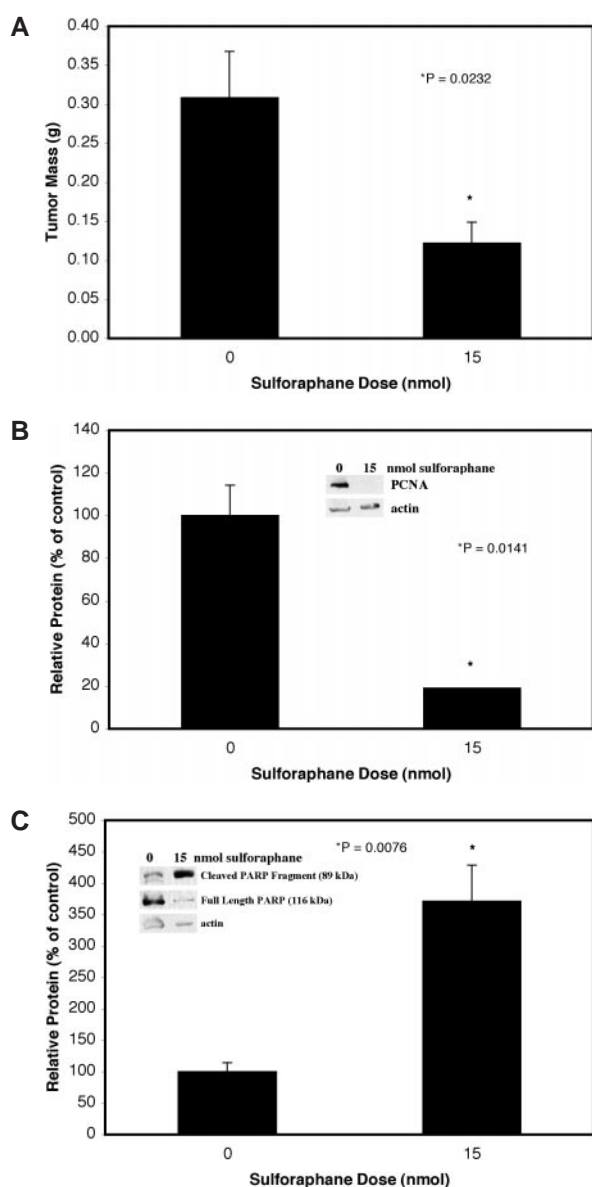


**Fig. 9.** Effect of SUL on implanted tumor cell growth in syngeneic BALB/c mice. Mean tumor mass (A) was significantly reduced ( $P < 0.05$ ) in SUL-treated animals, as compared with vehicle-administered controls. Western blot analysis of tumor protein samples indicated significantly ( $P < 0.05$ ) reduced PCNA (B) and elevated PARP fragment (C) in animals exposed to SUL.

expression, triggered caspase activation, reduced full-length PARP and induced condensation of nuclear chromatin. These results, together with the finding of elevated PARP fragment in tumors of animals dosed with SUL, strongly support the hypothesis that SUL acts to induce apoptosis. We also observed that SUL treatment was associated with accumulation of cells at  $G_2/M$ , which in part appeared to be due to mitotic arrest prior to metaphase. We infer this from our observations that SUL treatment was associated with *cdc2* kinase activation (Figure 3) and with distinguishable chromosomes scattered in a prophase- or prometaphase-like state (Figure 4C and E), without progression to the metaphase plate. Detailed characterization of the specific point of arrest in the  $G_2/M$  transition is warranted. Interestingly, while 15  $\mu M$  SUL did not lead to generalized depolymerization of cellular

microtubules, aberrant and mildly depolymerized mitotic spindles were observed (Figure 5F). Moreover, SUL at relatively high concentrations strongly inhibited tubulin polymerization *in vitro* (Figure 6), which suggests a mechanism of SUL-induced mitotic arrest involving altered tubulin polymerization and/or dynamics. Other naturally occurring anti-mitotic agents have been reported to trigger mitotic arrest via dose-dependent mechanisms involving tubulin disruption. For example, the *Vinca* alkaloid vinblastine has been shown to trigger mitotic block and disruption of microtubule dynamics at low doses, while relatively high doses are required for gross microtubule depolymerization (55). However, SUL like other isothiocyanates is a chemically reactive thiol and can inhibit numerous enzymes. Thus, the actions of SUL associated with progression from  $G_2$  through M-phase may be due to its effects on enzymes other than those involved in tubulin dynamics. Our data suggest a novel action of SUL, which needs to be characterized in greater detail.

Our findings with SUL in these cells add to an already considerable number of actions of SUL as an inhibitor of carcinogen activation by impeding CYP2E1 activity (8) and inducing phase II detoxification enzyme expression (7). Our data suggest that SUL may have heretofore unappreciated benefits in suppressing neoplastic breast cell proliferation and stimulating programmed cell death. Specifically, our data support the hypothesis that SUL acts as an inducer of mitotic catastrophe, which, unlike simple apoptosis, involves induction of a cell death pathway upon premature *cdc2* activation and/or inappropriate mitotic progression (14,15). For example, increased *cdc2* kinase activity has been reported to be requisite for the subsequent induction of cell death markers in MCF-7 human breast carcinoma cells by the anti-mitotic agent paclitaxel (56). We observed significant  $G_2/M$  accumulation as early as 2 h following SUL treatment (Figure 2B), along with cells exhibiting elevated *cdc2* kinase activity (Figure 3) and phenotypic evidence of mitotic arrest (Figure 4C and E) together with both morphological and molecular markers of apoptosis (aggregation of condensed nuclear chromatin, membrane blebbing, reduced Bcl-2 protein, caspase activation and depleted full-length PARP). This action of SUL on mitotic arrest and cell death warrants further characterization.

We have demonstrated SUL's efficacy as an anti-proliferative agent not only in cell culture, but also in the whole animal. BALB/c mice injected s.c. with F3II cells and subsequently injected daily i.v. with SUL were found to develop significantly smaller tumors (~60% less in mass), as compared with vehicle-administered controls (Figure 9A). It should be noted that subjects received i.v. SUL injections daily for 13 days and showed no outward signs of toxicity.

In conclusion, this study is the first to report the effectiveness of SUL as an inhibitor of mouse mammary carcinoma proliferation both *in vitro* and *in vivo*. The anti-proliferative mechanisms of this naturally occurring compound are several and include disruption of mitotic microtubules, *cdc2* kinase activation, and cell cycle arrest within  $G_2/M$ . These events occurred along with programmed cell death as characterized by decreased Bcl-2, increased caspase-3-like activity, and reduced full-length PARP. The *in vitro* anti-proliferative effect of SUL was confirmed in the whole animal in which growth of implanted breast cancer cells was significantly inhibited by SUL administration. Characterization of the nature of SUL's interaction with cellular targets responsible for facilitating

SUL-induced mitotic arrest will be of substantial interest in ultimately determining the potential of SUL as a chemopreventive and/or chemotherapeutic agent.

## Acknowledgements

We wish to express our sincere gratitude to Drs Jie Chen, Vladimir Gelfand (both in the Department of Cell and Structural Biology) and Joanne Messick (Department of Veterinary Clinical Medicine) at the University of Illinois for their excellent advice on control of cell cycle progression, microtubule structure and cytology of cell division, respectively. We also thank Dr John Bozzola, Director of Integrated Microscopy and Graphics Expertise (IMAGE) at Southern Illinois University, for technical advice and assistance with fluorescence microscopy. Supported by the University of Illinois Agricultural Experiment Station and United States Department of Agriculture National Needs Fellowship.

## References

- Gamet-Payraastre,L., Lumeau,S., Gasc,N., Cassar,G., Rollin,P. and Tulliez,J. (1998) Selective cytostatic and cytotoxic effects of glucosinolates hydrolysis products on human colon cancer cells *in vitro*. *Anticancer Drugs*, **9**, 141–148.
- Faulkner,K., Mithen,R. and Williamson,G. (1998) Selective increase of the potential anticarcinogen 4-methylsulphanylbutyl glucosinolate in broccoli. *Carcinogenesis*, **19**, 605–609.
- Freundenheim,J.L., Marshall,J.R., Vena,J.E., Laughlin,R., Brasure,J.R., Swanson,M.K., Nemoto,T. and Graham,S. (1996) Premenopausal breast cancer risk and intake of vegetables, fruits and related nutrients. *J. Natl Cancer Inst.*, **88**, 340–348.
- Franceschi,S., Parpinel,M., La Vecchia,C., Favero,A., Talamini,R. and Negri,E. (1998) Role of different types of vegetables and fruit in the prevention of cancer of the colon, rectum and breast. *Epidemiology*, **9**, 338–341.
- Franceschi,S., Favero,A., Carlo,L.V., Negri,E., Luigino,D.M., Salvini,S., Decarli,A. and Giacosa,A. (1995) Influence of food groups and food diversity on breast cancer risk in Italy. *Int. J. Cancer*, **63**, 785–789.
- Zhang,Y., Kensler,T.W., Cho,C.-G., Posner,G.H. and Talalay,P. (1994) Anticarcinogenic activities of sulforaphane and structurally related synthetic norbornyl isothiocyanates. *Proc. Natl Acad. Sci. USA*, **91**, 3147–3150.
- Zhang,Y., Talalay,P., Cho,C.-G. and Posner,G.H. (1992) A major inducer of anticarcinogenic protective enzymes from broccoli: Isolation and elucidation of structure. *Proc. Natl Acad. Sci. USA*, **89**, 2399–2403.
- Barcelo,S., Gardiner,J.M., Gescher,A. and Chipman,J.K. (1996) CYP2E1-mediated mechanism of anti-genotoxicity of the broccoli constituent sulforaphane. *Carcinogenesis*, **17**, 277–282.
- Gamet-Payraastre,L., Li,P., Lumeau,S., Cassar,G., Dupont,M.-A., Chevolleau,S., Gasc,N., Tuilliez,J. and Terce,F. (2000) Sulforaphane, a naturally occurring isothiocyanate, induces cell cycle arrest and apoptosis in HT29 colon cancer cells. *Cancer Res.*, **60**, 1426–1433.
- Huang,C., Ma,W.Y., Li,J., Hecht,S.S. and Dong,Z. (1998) Essential role of p53 in phenethyl isothiocyanate-induced apoptosis. *Cancer Res.*, **58**, 4102–4106.
- Yu,R., Mandlekar,S., Harvey,K.J., Ucker,D.S. and Kong,A.N. (1998) Chemopreventive isothiocyanates induce apoptosis and caspase-3-like protease activity. *Cancer Res.*, **58**, 402–408.
- Moreno,S., Hayles,J. and Nurse,P. (1989) Regulation of p34cdc2 protein kinase during mitosis. *Cell*, **58**, 361–372.
- Th'ng,J.P.H., Wright,P.S., Hamaguchi,J., Lee,M.G., Norbury,C.J., Nurse,P. and Bradbury,E.M. (1990) The FT210 cell line is a mouse G<sub>2</sub> phase mutant with a temperature-sensitive CDC2 gene product. *Cell*, **63**, 313–324.
- Chan,T.A., Hermeeking,H., Lengauer,C., Kinzler,K.W. and Vogelstein,B. (1999) 14-3-3Sigma is required to prevent mitotic catastrophe after DNA damage. *Nature*, **401**, 616–620.
- Shi,L., Nishioka,W.K., Th'ng,J., Bradbury,E.M., Litchfield,D.W. and Greenberg,A.H. (1994) Premature p34cdc2 activation required for apoptosis. *Science*, **263**, 1143–1145.
- Krek,W. and Nigg,E.A. (1991) Differential phosphorylation of vertebrate p34cdc2 kinase at the G<sub>1</sub>/S and G<sub>2</sub>/M transitions of the cell cycle: identification of major phosphorylation sites. *EMBO J.*, **10**, 305–316.
- Gould,K.L., Moreno,S., Owen,D.J., Sazer,S. and Nurse,P. (1991) Phosphorylation at Thr167 is required for *Schizosaccharomyces pombe* p34cdc2 function. *EMBO J.*, **10**, 3297–3309.
- Norbury,C., Blow,J. and Nurse,P. (1991) Regulatory phosphorylation of the p34cdc2 protein kinase in vertebrates. *EMBO J.*, **10**, 3321–3329.
- Norbury,C. and Nurse,P. (1992) Animal cell cycles and their control. *Annu. Rev. Biochem.*, **61**, 441–470.
- Gautier,J., Minshull,J., Lohka,M., Glotzer,M., Hunt,T. and Maller,J.L. (1990) Cyclin is a component of maturation-promoting factor from xenopus. *Cell*, **60**, 487–494.
- Solomon,M.J., Glotzer,M., Lee,T.H., Philippe,M. and Kirschner,M.W. (1990) Cyclin activation of p34cdc2. *Cell*, **63**, 1013–1024.
- Labbe,J.-C., Capony,J.-P., Caput,D., Cavadore,J.-C., Derancourt,J., Kaghad,M., Lelias,J.-M., Picard,A. and Doree,M. (1989) MPF from starfish oocytes at first meiotic metaphase is a heterodimer containing one molecule of cdc2 and one molecule of cyclin B. *EMBO J.*, **8**, 3053–3058.
- McGowan,C.H. and Russell,P. (1993) Human Wee1 kinase inhibits cell division by phosphorylating p34cdc2 exclusively on Tyr15. *EMBO J.*, **12**, 75–85.
- Parker,L.L., Atherton-Fessler,S., Lee,M. S., Ogg,S., Falk,J.L., Swenson,K.I. and Piwnica-Worms,H. (1991) Cyclin promotes the tyrosine phosphorylation of p34cdc2 in a wee1+ dependent manner. *EMBO J.*, **10**, 1255–1263.
- Russell,P. and Nurse,P. (1987) Negative regulation of mitosis by wee1+, a gene encoding a protein kinase homolog. *Cell*, **49**, 559–567.
- McGowan,C.H. and Russell,P. (1995) Cell cycle regulation of human WEE1. *EMBO J.*, **14**, 2166–2175.
- Watanabe,N., Broome,M. and Hunter,T. (1995) Regulation of the human WEE1Hu CDK tyrosine 15-kinase during the cell cycle. *EMBO J.*, **14**, 1878–1891.
- Lundgren,K., Walworth,N., Booher,R., Dembski,M., Kirschner,M. and Beach,D. (1991) mik1 and wee1 cooperate in the inhibitory tyrosine phosphorylation of cdc2. *Cell*, **64**, 1111–1122.
- Mueller,P.R., Coleman,T.R., Kumagai,A. and Dunphy,W.G. (1995) Myt1: a membrane-associated inhibitory kinase that phosphorylates CDC2 on both threonine-14 and tyrosine-15. *Science*, **270**, 86–90.
- Lee,M.S., Ogg,S., Xu,M., Parker,L.L., Donoghue,D.J., Maller,J.L. and Piwnica-Worms,H. (1992) cdc25+ encodes a protein phosphatase that dephosphorylates p34cdc2. *Mol. Biol. Cell*, **3**, 73–84.
- Millar,J.B., McGowan,C.H., Lenaers,G., Jones,R. and Russell,P. (1991) p80cdc25 mitotic inducer is the tyrosine phosphatase that activates p34cdc2 kinase in fission yeast. *EMBO J.*, **10**, 4301–4309.
- Kumagai,A. and Dunphy,W.G. (1991) The cdc25 protein controls tyrosine dephosphorylation of the cdc2 protein in a cell-free system. *Cell*, **64**, 903–914.
- Langan,T.A., Gautier,J., Lohka,M., Hollingsworth,R., Moreno,S., Nurse,P., Maller,J. and Sclafani,R.A. (1989) Mammalian growth-associated H1 histone kinase: a homolog of cdc2+/CDC28 protein kinases controlling mitotic entry in yeast and frog cells. *Mol. Cell. Biol.*, **9**, 3860–3868.
- Peter,M., Nakagawa,J., Doree,M., Labbe,J.C. and Nigg,E.A. (1990) Identification of major nucleolar proteins as candidate mitotic substrates of cdc2 kinase. *Cell*, **60**, 791–801.
- Luscher,B., Brizuela,L., Beach,D. and Eisenman,R.N. (1991) A role for the p34cdc2 kinase and phosphatases in the regulation of phosphorylation and disassembly of lamin B2 during the cell cycle. *EMBO J.*, **10**, 865–875.
- Ward,G.E. and Kirschner,M.W. (1990) Identification of cell cycle-regulated phosphorylation sites on nuclear lamin C. *Cell*, **61**, 561–577.
- Heald,R. and McKeon,F. (1990) Mutations of phosphorylation sites in lamin A that prevent nuclear lamina disassembly in mitosis. *Cell*, **61**, 579–589.
- Peter,M., Nakagawa,J., Doree,M., Labbe,J.C. and Nigg,E.A. (1990) *In vitro* disassembly of the nuclear lamina and M phase-specific phosphorylation of lamins by cdc2 kinase. *Cell*, **61**, 591–602.
- Chou,Y.-H., Bischoff,J.R., Beach,D. and Goldman,R.D. (1990) Intermediate filament reorganization during mitosis is mediated by p34cdc2 phosphorylation of vimentin. *Cell*, **62**, 1063–1071.
- Yamashiro,S., Yamakita,Y., Hosoya,H. and Matsumura,F. (1991) Phosphorylation of non-muscle caldesmon by p34cdc2 kinase during mitosis. *Nature*, **349**, 169–172.
- Belenguer,P., Caizergues-Ferrer,M., Labbe,J.-C., Doree,M. and Amalric,F. (1990) Mitosis-specific phosphorylation of nucleolin by p34cdc2 protein kinase. *Mol. Cell. Biol.*, **10**, 3607–3618.
- Lorca,T., Labbe,J.C., Devault,A., Fesquet,D., Capony,J.P., Cavadore,J.C., Le Bouffant,F. and Doree,M. (1992) Dephosphorylation of cdc2 on threonine 161 is required for cdc2 kinase inactivation and normal anaphase. *EMBO J.*, **11**, 2381–2390.

43. Glotzer, M., Murray, A.W. and Kirschner, M.W. (1991) Cyclin is degraded by the ubiquitin pathway. *Nature*, **349**, 132–138.
44. Fotodar, R., Flatt, J., Gupta, S., Margolis, R. L., Fitzgerald, P., Messier, H. and Fotodar, A. (1995) Activation-induced T-cell death is cell cycle dependent and regulated by cyclin B. *Mol. Cell. Biol.*, **15**, 932–942.
45. Kroemer, G. (1997) The proto-oncogene Bcl-2 and its role in regulating apoptosis. *Nature Med.*, **3**, 614–620.
46. Oltersdorf, T. and Fritz, L.C. (1998) The Bcl-2 family: targets for the regulation of apoptosis. In Bristol, J.A. (ed.) *Annual Reports In Medicinal Chemistry*. Academic Press, San Diego, Vol. 33, pp. 253–262.
47. Zha, H., Aime-Sempe, C., Sato, T. and Reed, J.C. (1996) Proapoptotic protein Bax heterodimerizes with Bcl-2 and homodimerizes with Bax via a novel domain (BH3) distinct from BH1 and BH2. *J. Biol. Chem.*, **271**, 7440–7444.
48. Zoltan, O., Milliman, C.L. and Korsmeyer, S.J. (1993) Bcl-2 heterodimerizes *in vivo* with a conserved homolog, Bax, that accelerates programmed cell death. *Cell*, **74**, 609–619.
49. Zha, H., Fisk, H.A., Yaffe, M.P., Mahajan, N., Herman, B. and Reed, J.C. (1996) Structure-function comparisons of the proapoptotic protein Bax in yeast and mammalian cells. *Mol. Cell. Biol.*, **16**, 6494–6508.
50. Porter, A.G. (1999) Protein translocation in apoptosis. *Trends Cell Biol.*, **9**, 394–401.
51. Zornig, M., Hueber, A.-O., Baum, W. and Evan, G. (2001) Apoptosis regulators and their role in tumorigenesis. *Biochim. Biophys. Acta*, **1551**, F1–F37.
52. Thornberry, N.A. and Lazebnik, Y. (1998) Caspases: enemies within. *Science*, **281**, 1312–1316.
53. Casciola-Rosen, L., Nicholson, D.W., Chong, T., Rowan, K.R., Thornberry, N.A., Miller, D.K. and Rosen, A. (1996) Apopain/CPP32 cleaves proteins that are essential for cellular repair: a fundamental principle of apoptotic death. *J. Exp. Med.*, **183**, 1957–1964.
54. Hu, C.C., Tang, C.H. and Wang, J.J. (2001) Caspase activation in response to cytotoxic *Rana catesbeiana* ribonuclease in MCF-7 cells. *FEBS Lett.*, **503**, 65–68.
55. Jordan, M. A. (2002) Mechanism of action of antitumor drugs that interact with microtubules and tubulin. *Curr. Med. Chem. Anti-Cancer Agents*, **2**, 1–17.
56. Shen, S.C., Huang, T.S., Jee, S.H. and Kuo, M.L. (1998) Taxol-induced p34cdc2 kinase activation and apoptosis inhibited by 12-*O*-tetradecanoylphorbol-13-acetate in human breast MCF-7 carcinoma cells. *Cell Growth Differ.*, **9**, 23–29.

Received July 3, 2003; revised September 29, 2003; accepted October 3, 2003